16th World Conference on Earthquake Engineering, 16WCEE 2017
Santiago Chile, January 9th to 13th 2017
Paper N° 4705
Registration Code: S-K1466089507

A loss-based control algorithm for magnetorheological dampers combined with earthquake early warning

O. Velazquez[(1)], C. Galasso[(2)], P. Duffour[(3)]

[(1)] PhD Student, Institute for Risk and Disaster Reduction and Dept. of Civil, Environmental & Geomatic Engineering, University College London, London, UK, omar.velazquez@ucl.ac.uk
[(2)] Lecturer, Institute for Risk and Disaster Reduction and Dept. of Civil, Environmental & Geomatic Engineering, University College London, London, UK, c.galasso@ucl.ac.uk
[(3)] Lecturer, Dept. of Civil, Environmental & Geomatic Engineering, University College London, London, UK, p.duffour@ucl.ac.uk

Abstract

This paper presents a methodology that combines the use of magnetorheological (MR) dampers together with an earthquake early warning (EEW) system to minimize the losses in a structure about to be struck by an incoming ground motion. MR dampers can generate relatively large controllable damping forces by tuning the viscosity of an MR fluid through a control voltage. Their mechanical simplicity, fast response time, and low electric power requirements make them attractive for potential applications in earthquake engineering, particularly when combined with EEW.

In this paper, a control algorithm is developed to determine the command voltage of the MR damper based on the expected ground shaking predicted by an EEW system. A general framework is introduced that develops a performance-based (i.e., loss-based) control algorithm for semi-active devices combined with an EEW system. A simplified story-based building-specific component-based loss estimation is used in the proposed framework, combining real-time, EEW-based seismic hazard, nonlinear dynamic structural simulation, damage fragility and loss. For illustrative purposes, the control algorithm is implemented on a generic three-story building structure equipped with a small-scale MR damper prototype.

Results reveal that the developed EEW-based control algorithm can effectively reduce the expected loss of the considered case-study structure.

Keywords: Semi-Active Control, Earthquake Early Warning, MR Damper, Performance Based Earthquake Engineering

1. Introduction

The goal of an earthquake early warning (EEW) system is to detect earthquakes in the early stages of fault rupture, rapidly predict the intensity of the subsequent ground motion, and warn end-users before they experience the strong shaking that might cause damage. The most damaging shaking is usually caused by seismic shear (or S-) and surface waves, which travel at about half the speed of the fastest waves (primary waves; or P-waves), and much slower than an electronic warning signal (which travel at nearly the speed of light). EEW systems use P-waves (or early portions of S-waves) to detect strong shaking at an earthquake's epicenter and transmit alerts ahead of the damaging S-waves [1]. EEW systems can provide up to a few tens of seconds of warning prior to the arrival of damaging ground shaking at a target site. The warning time depends on the distance to the earthquake epicenter. This allows for real-time seismic risk-mitigating actions, including alerting people to “drop, cover, and hold-on" or move to safer locations, as well as many types of automated actions such as stopping elevators at the nearest floor, opening firehouse doors, slowing rapid-transit vehicles and high-speed trains to avoid accidents, shutting down pipelines and gas lines to minimize fire hazards, shutting down manufacturing operations to decrease potential damage to equipment, saving vital computer information to avoid data losses, etc. From the engineering perspective, if an earthquake is going to strike a target structure (or infrastructure/infrastructure component) and induce a response of sufficient severity, then planned mitigating actions (alerting occupants, controlling elevators, etc.) can be taken immediately in order to limit potential losses.

In practice, two fundamental problems in EEW restrict its applications: short warning time, particularly close to the epicenter, and large uncertainty on the predicted ground motion [2]. EEW information always involves some uncertainty and some EEW applications may lead to a substantial economic loss if a false alarm occurs [3]. Therefore, deciding whether to take mitigation actions should be based on an advanced loss analysis. Moreover, as the available warning time is short, human intervention would likely take too long for any actions from being activated in a timely manner. Therefore, automated decision and mitigation actions are favored.

Some recent studies (e.g., [4]) have discussed the semi-active control of structures as a possible advanced engineering application of EEW, especially in areas where the available warning time is very short (near the so-called *blind-zone*). In this scenario, a building can change its dynamic properties within a few seconds (or milliseconds) to better withstand the approaching ground shaking. The combined use of EEW and structural control may reduce the structural vulnerability (and resulting losses) of specific systems, for example critical infrastructure such as hospitals, fire stations, networks, etc., which have to be operational for emergency management purposes during or right after the event. As earthquakes often affect power supplies, semi-active devices are a sensible option for seismic mitigation as they can easily operate on back-up power. However, one of the key issues in using EEW with semi-active control is to properly account for the uncertainty in the EEW-based estimation of the event features: the effectiveness of such applications greatly depends on the quality of the pre-arrival ground motion information provided by the EEW system.

In this study, magnetorheological (MR) dampers are proposed to change the mechanical properties of a hosting structure according to information on an incoming earthquake provided by an EEW system. In particular, this paper proposes a loss-based probabilistic framework to derive an optimum structural control strategy minimizing potential losses from an incoming earthquake.

The present paper is organized as follows. First, the basic concepts of (1) Real-Time Probability Seismic Hazard Analysis (RTPSHA) for EEW applications; and (2) structural control, with special focus on MR dampers, are provided. Next, the proposed loss-based control algorithm for MR dampers combined with EEW is described, followed by the description of the illustrative example used in the paper. The final sections discuss the results and offer some conclusions.

2. Background

2.1 Real-Time Probabilistic Seismic Hazard Analysis (RTPSHA)

A regional EEW system is based on a dense sensor network covering a geographical area of high seismicity. When an earthquake occurs, the relevant source parameters (event location and magnitude) are estimated from the early portion of recorded signals (initial P-waves) at sensors closest to the epicenter. The estimated source parameters can then be used to predict, with quantified confidence, a ground motion intensity measure (IM) at a distant site where a target structure of interest is located. Specifically, recent efforts of real-time seismology on rapid assessment of earthquake magnitude and location [1] enable to provide an estimate of the event's features from a few seconds to a few tens of seconds before the ground motion arrives at a target site. When an event occurs, probabilistic distributions of magnitude (M) and source-to-site distance (R) are available, conditional on some parameters measured in the early portion of the P- (and sometimes S-) wave trains at a number of near-source stations. These parameters are generally associated with the low-frequency content of the data, which is sensitive to the seismic moment, and can be related to the maximum amplitude, the dominant frequency or the energy released by the event ([1], for a comprehensive review of these parameters and related EEW models). The prediction of different IMs, conditional on those parameters, may be performed by analogy to the well-known probabilistic seismic hazard analysis (PSHA) but in real-time ([3] and [5]) as formulated in Eq. (1).

$$f_{IM,n}(IM \mid \underline{\tau},\underline{s}) = \iint_{m\,r} f_{IM}(IM \mid m,r)\, f_M(m \mid \underline{\tau})\, f_R(r \mid \underline{s})\, dm\, dr\,, \tag{1}$$

where $f_R(r \mid \underline{s})$ is the probability density function (PDF) of R conditional on the sequence according to which n stations triggered (at a given time t), $\underline{s} = \{s_1, s_2, ..., s_n\}$, $f_M(m \mid \underline{\tau})$ is the PDF of M conditional on the measures from the n stations triggered (at t), $\underline{\tau} = \{\tau_1, \tau_2, ..., \tau_n\}$, and can be expressed analytically using Bayes' theorem [3]; $f_{IM}(IM \mid m,r)$ is the PDF of the considered IM conditional on M and R, e.g., from a ground motion prediction equation (GMPE). The vector $\underline{\tau} = \{\tau_1, \tau_2, ..., \tau_n\}$ may include any possible parameter estimated from the early portion of recorded signal. It was shown in [6] that $f_M(m \mid \underline{\tau})$ depends on the measures only via the summation of the logs, $\hat{\tau} = \sum_{i=1}^{n} \ln(\tau_i)$ and n. The modal value of R alone may adequately represent its PDF due to the negligible uncertainty involved in the earthquake location rapid estimation methods. Therefore, because the GMPE is a static piece of information (not depending on the real-time measures), the RTPSHA integral may be computed offline for all possible values of the $\hat{\tau}$ and R pair, and the result has only to be retrieved in real-time without the need for computing it. This is an attractive feature of the proposed approach [7].

Eq. (1) results time-dependent hazard curves which may be used as a support tool for automated decision-making to reduce the expected loss of specific structures/infrastructures in the framework of performance-based earthquake engineering (PBEE), even in those cases where limited lead-time renders evacuation unfeasible. However, real-time IMs predictions are performed in very uncertain conditions linked to both the real-time estimation of source parameters and the traditional uncertainties involved in PSHA (e.g., [8]).

2.2 Structural Control

Structural control is an additional tool that can be used to meet desired performance objectives, within the framework of PBEE. Over the past decades, several control devices and algorithms have been proposed to mitigate the dynamic response of a structure during extreme events such as earthquakes and strong winds [9].

There are mainly three classes of control devices. Passive devices, which require no external power, are reliable and never destabilize the structure. Such devices basically reduce the seismic demand on the structure either by increasing the energy dissipation potential (i.e., increasing structural damping) and/or by changing its fundamental oscillation period moving it away from the most energetic frequency content of ground motion (e.g., seismic base isolation). However, they have low adaptability if the actual external loading conditions or usage patterns are different from those they were designed for. This makes integrating EEW with passive control

systems difficult. On the other hand, active control devices are adaptive to varying usage patterns and loading conditions. Such devices supply control forces based on feedback from sensors (located near to/on the structure) that measure the excitation and/or the actual response. The recorded measurements from the response and/or excitation are processed by a controller which, based on an algorithm, operates actuators producing the forces. However, generating control forces by electromechanical or hydraulic actuators requires power sources of the order of tens of kilowatts for small structures and may reach several megawatts for large structures. This, together with their stability problems and overall reliability are still major concerns to engineers. Moreover, active control strategies are usually based on information about the full waveform or structural response which cannot be predicted by EEW.

Semi-active devices, combining the versatility and adaptability of the active devices and the reliability of the passive devices, have attracted considerable attention for the seismic protection of structures in recent years [9]–[12]. These devices develop control forces based on the feedback from sensors that measure the excitation and/or the response of the structure and do not input energy to the structure (so, they usually do not induce adverse effect on the stability of the structure). The stiffness and/or damping properties of a structure can be adjusted according to the instantaneous (measured) response of the hosting structure (feed-back) and/or to the instantaneous (measured) properties of the earthquake input (feed-forward). In both cases, a control algorithm describes the relationship between the observed quantities (e.g., displacements/velocities/accelerations of the structure, accelerations of the ground) and the corresponding optimal values of stiffness and damping (which can be changed by means of electrical signals) of the adjustable devices. The energy required for the modification of the basic parameters of a semi-active device is small compared to that needed to operate conventional actuators (generally approximately tens of watts, so it can be supplied by simple batteries - e.g., to open/close a valve).

Several strategies have been proposed to control the behavior of semi-active devices (e.g., [11]). Each of the proposed control strategies has its own merits and limitations depending on the specific application and desired performance. Comparative studies are needed to evaluate the performance of each control method. As an example, [13] described a methodology, referred to as *probabilistic seismic control analysis*, for the development of probabilistic seismic demand curves for structures with supplemental control devices. The proposed methodology is applied to case-study structures (3- and 9-story) equipped with three different control systems, namely (i) base isolation (passive), (ii) linear viscous brace dampers (passive); and (iii) active tendon braces. Results from this study indicated that no single control strategy is the most effective for all the hazard levels/return periods.

2.2.1 MR dampers

One of the most promising semi-active devices is the MR damper. These are semi-active damping devices first investigated in the context of civil engineering by Dyke et al. [10]. A magnetorheological fluid is an oily liquid containing iron micro-filings. When no magnetic field is present, the iron particles are randomly dispersed in the fluid and affects little its underlying viscosity. When the MR fluid is subjected to a magnetic field, the iron micro-particles align and form linear chains which increase the fluid viscosity by several orders of magnitude. Like conventional viscous dampers, MR dampers consist of a fluid-filled cylindrical chamber along which a tightly fitting piston moves. In this case, however, the chamber is filled with MR fluid and is wrapped within an electric coil. Supplying the coil with a current induces a magnetic field in the fluid and changes its viscosity. By varying the current in the coil (through an input voltage), the magnitude of the force developed in the damper can be controlled. MR dampers adapt with very fast response times (i.e., < 1s including trigger and set up time [14]) over a broad temperature range and have low power requirements. They are relatively inexpensive to manufacture and maintain. During the last few decades researchers have investigated both numerically and experimentally the behavior of MR dampers and semi-active control algorithms associated with these types of dampers for earthquake hazard mitigation [15]. Fig. 1 shows the force-displacement and force-velocity loops for a small-scale prototype MR damper subjected to harmonic cycles (constant amplitude of 1.5 cm and frequency of 2.5 Hz) for varying input voltage levels. It is clear from these graphs that MR damper behavior is highly nonlinear and voltage-dependent.

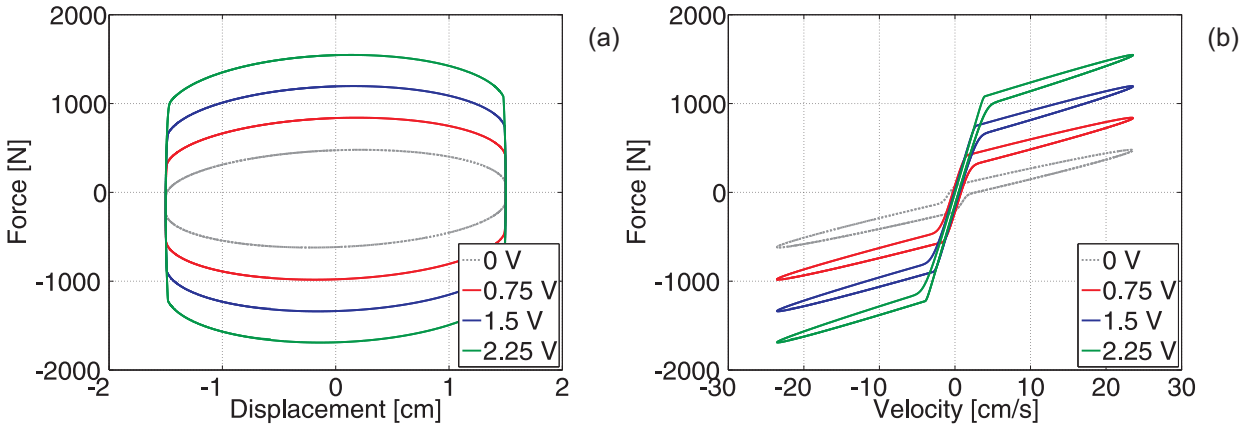

Fig. 1 – Force-displacement (a) and force-velocity (b) loops for a small-scale prototype MR damper for imposed harmonic cycles at different current levels.

For structural control MR dampers can be used either in passive or semi-active mode. In passive mode, illustrated in the block diagram shown in Fig. 2a, a constant current is supplied to the MR damper. No feedback data are required and the damper force is generated passively by the movement of the damper. In the remainder of the paper, passive-on and passive-off controls refer to the cases when the maximum and no current, respectively, are supplied to the damper.

The semi-active controlled system shown in Fig. 2b uses feedback data, requiring the use of sensors (e.g., accelerometers, load cells, displacement transducers), and a controller to determine the damper control force.

A basic semi-active control algorithm is based on the simple on/off command current rule. The state of the structure is assessed and the controller determines if increasing the damper force is beneficial to reduce the response of the structure. If so, the semi-active controller inputs the maximum current (i.e., on-mode) to the damper to maximize the benefit. Otherwise, it just inputs the minimum current (i.e., off-mode).

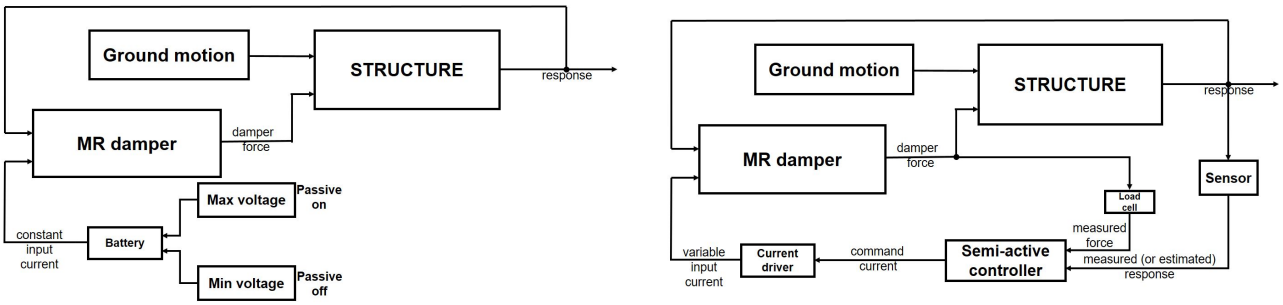

Fig. 2 - Block diagram for a passive controlled system with MR damper (left); Block diagram for a semi-active controlled system with MR damper (right; adapted from [16]).

More sophisticated control algorithms can be used to control MR dampers (e.g., decentralized bang-bang Control, Maximum Energy Dissipation, Clipped-Optimal Control [17]). Following [18], this study uses MR Dampers in a “passive smart” mode: the mechanical properties of the device are set just before the arrival of a seismic event at a site, according to the IM estimate of the incoming earthquake provided by the geographically relevant EEW system (Fig. 3). This adjustment is supposed to only happen once, keeping the device control parameter unaltered for the whole duration of the seismic event. In this publication, this control strategy is referred as ‘SA+EEW’. Later in the paper it will be compared to the passive strategy (coil fed with the maximum voltage) and a semi-active strategy proposed by [12] called the Improved-Clipped Algorithm ('SA ICA'). 'SA ICA' represents an improvement of the clipped-optimal control algorithms for MR dampers introduced by [14].

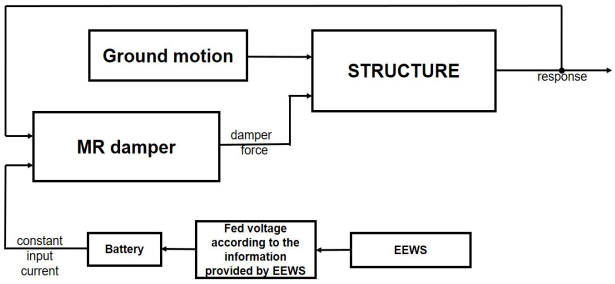

Fig. 3 - Block diagram for a smart passive controlled system with MR damper combined with EEW.

It is worth noting that the study presented in [19] has several limitations which are addressed here: the peak ground acceleration (PGA) is used as the selected IM in their study, stating that 'the research to reliably predict the complete elastic spectrum is still in progress', not considering the study of [5]; only 16 ground motion records were used in the calibration of the control algorithm based on EEW, with low statistical significance of the presented results; the uncertainty analysis performed to investigate the sensitivity of the results to uncertainty in the EEW real-time estimates is based on simplified assumptions/models; the control algorithm is based on the reduction of peak response quantities of a benchmark highway bridge rather than in terms of expected loss. This last point is particularly important: the designed algorithm should provide the optimal value of voltage that would provide the optimal structural response considering all the EDPs of interest. Given that different EDPs represent different physical quantities (with different units) and show different trends as function of the input voltage in the MR damper, a loss-based algorithm is the only option able to incorporate the representative contribution of all the EDPs taken into consideration.

3. Loss-Based Control Algorithm for MR dampers

The loss estimation approach used in this study is primarily based on the simplified story-based building-specific loss estimation method proposed in [19]. To develop a building-specific relationship linking ground motion with an intensity level of IM to the expected economic monetary loss (L), Eq. (2) can be used:

$$E[L \mid IM] = E[L \mid NC, IM]P(NC \mid IM) + E[L \mid C]P(C \mid IM), \quad (2)$$

where $E[L \mid NC, IM]$ is the expected loss in the building given that collapse has not occurred at the given IM level; $E[L \mid C]$ is the expected loss given that the building has collapsed (i.e., cost of removal of debris from the site plus replacement value); $P(NC \mid IM)$ is the probability that the building does not collapse at the given IM level; and $P(C \mid IM)$ is the probability the building does collapse at the given IM level (which is complementary to $P(NC \mid IM)$, i.e., $P(NC \mid IM) = 1 - P(C \mid IM)$). $P(C \mid IM)$ can be quantified by using nonlinear structural simulation (e.g., [20]); in this study, $P(C \mid IM)$ is determined using the results of nonlinear dynamic analysis by establishing a collapse criteria based on maximum interstory drift ratio (MIDR), i.e., collapse occurs if MIDR is larger than 10%. At this level of deformation, it is assumed that the building will not be able to recover a stable position and side-sway collapse will be initiated.

$E[L \mid NC, IM]$ in Eq. (2) can be computed using a story-based approach by grouping individual component losses per story and pre-computing estimated damage using assumed cost distribution of the total story value, Eqs. (3) to (5):

$$E[L \mid NC, IM] = \sum_{i=1}^{\#story} \sum_{k=1}^{3} E[L_{i,k} \mid NC, IM], \quad (3)$$

$$E[L_{i,k} \mid NC, IM] = \int_{edp} E[L_{i,k} \mid NC, EDP_k] \left| dP(EDP_k > edp_k \mid NC, IM) \right|, \quad (4)$$

$$E\left[L_{i,k} \mid NC, EDP_k\right] = \sum_{j=1}^{\#DS} E\left[L_{i,k} \mid DS = ds_j\right] P\left(DS = ds_j \mid NC, EDP_k\right). \quad (5)$$

In Eq. (4), $E\left[L_{i,k} \mid NC, IM\right]$ is the expected loss (eventually normalized by the original cost of the component or its replacement value) at the *i*-th story for the *k*-th component category given that collapse has not occurred at the given IM level; $E\left[L_{i,k} \mid NC, EDP_k\right]$ is the expected loss (normalized by the original cost of the component) at the *i*-th story for the *k*-th component category conditional on non-collapse and the Engineering Demand Parameter (EDP) associated with the *k*-th component category $\left(EDP_k\right)$; and $P\left(EDP_k > edp_k \mid NC, IM\right)$ is the complementary cumulative distribution function (CCDF) of EDP_k conditional on non-collapse and the given IM level and can be computed by using nonlinear structural simulation (e.g., [21]). In Eq. (5), $E\left[L_{i,k} \mid DS = ds_j\right]$ is the expected loss (eventually normalized by the original cost of the component) at the *i*-th story for the *k*-th component category given that collapse has not occurred at the given damage state $\left(ds_j\right)$; $P\left(DS = ds_j \mid NC, EDP_k\right)$ is the probability of being at (or exceeding) a damage state ds_j conditional on the EDP level associated with the *k*-th component category (i.e., component-specific fragility functions, see e.g. [22]).

The seismic demand (in terms of an EDP) due to seismic excitation can be estimated by performing a Probabilistic Seismic Demand Analysis (PSDA) on a computational model of the building. One possible approach in PSDA (used in this study) is to apply a series of earthquake ground motion time histories to the building model and to estimate the peak responses at different levels along the building height. For the purpose of loss estimation described above, the structural response has to be evaluated at all stories in terms of the EDPs that have the closest correlation with the damage in the components. Three broad categories of components are considered here: (1) drift-sensitive structural components; (2) drift-sensitive non-structural components; and (3) acceleration-sensitive components. Hence, an inventory of components and their location within the structure is required.

The main output from PSDA is the probability distribution of the structural response, namely interstory drift ratio (IRD) and peak floor acceleration (PFA), at different locations and at different levels of intensity. For each category of components, fragility functions can be used to estimate the probability that a particular building component will reach or exceed different damage states as a function of the EDPs. The repair or replacement cost of a component can finally be estimated by itemizing the tasks that need to be accomplished after the occurrence of each of the damage states.

The main objective of the approach proposed here is to set the input voltage u to the MR damper, within the range 0-u_{max}, according to a given control algorithm u(IM) so as to obtain the minimum expected loss during the seismic excitation. The given IM value to input into the control algorithm can be the expected value of the real-time distribution of the considered IM (derived through the RTPSHA).

To calibrate the u(IM) algorithm, a set of nonlinear time-history analyses can be performed using a set of (unscaled) ground motion records; for each ground motion record, the MR damper is fed with a range of voltage values (0-u_{max} with a given step Δu), always keeping the input voltage constant for the whole duration of the event. For each ground motion, the value of the different EDPs is computed (for each voltage) and the optimal value of voltage u_{opt} – the one leading to the minimum expected loss – is recorded. Eq. (5) is used to estimate each component expected loss (at each story) as a function of the EDP (corresponding to a given ground motion record - characterized by a given IM and voltage value) and to select u_{opt} for the given IM. Robust regression can be finally used to fit an analytical control model to the obtained (IM, u_{opt}) values.

Eqs. (3) and (4) can be used to estimate the component expected loss (at each story) and the total expected loss as a function of the level of intensity IM. This result can be used to compare the expected loss for different control strategies for different hazard levels and test the effectiveness of the proposed integration between smart passive MR damper and EEW.

4. Case-study

A numerical example is presented in this section to illustrate how to implement the loss-based control algorithm for MR dampers combined with EEW, as discussed above. The numerical example consists of a scaled three-story building structures modelled in Simulink® as a simple three-degree-of-freedom shear frame. It is fitted with an MR damper connecting the ground and first floor (Fig. 4a). The location(s) for the control devices in the structure could be changed to optimize the structural performance but the particular topology shown in Fig. 4a is adopted because it has been widely used by other researchers testing different control strategies employing MR dampers in the past (e.g., [12]). The structure has a fundamental period T_1 equal to 0.2s.

The MR damper used in this study is a small-scale 3000N prototype similar to the one used by Dyke et al in [10]. It is based on a commercially available device. Although small by civil engineering standards, experimental test data and model validation studies are available in the literature (e.g. [12]) which could be used to calibrate our model. The input current for the considered damper is 0-1 amp, which is proportional to an applied voltage input of 0-3V. The MR damper and control model used in this paper have a maximum voltage of 2.25V (0.75 amp) as the experimental data available suggests saturation above this value.

The modified Bouc-Wen model shown diagrammatically in Fig. 4b is a general parametric mathematical model that allows general hysteresis behaviors to be simulated. Many previous studies on MR dampers have shown that it can model accurately their hysteretic behavior [17], therefore it was chosen in this study to simulate the device. The model parameters of the MR damper governing equations are function of the applied voltage, *u*. Details on the MR damper parameters used in this simulation are those used in [12]. Force-Displacement and Force-Velocity plots of the Bouc-Model were shown in Fig. 1.

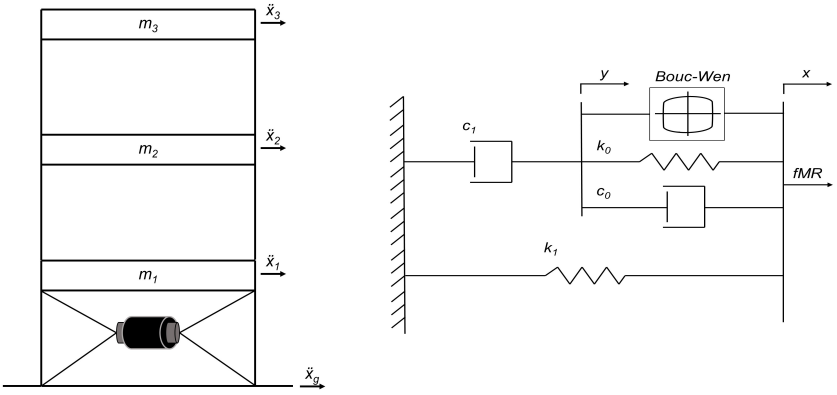

Fig. 4 – Case-study structure (left); Modified Bouc-Wen model for MR dampers (right).

A set of 150 unscaled ground motion records from the SIMBAD database (Selected Input Motions for Displacement-Based Assessment and Design [24]), is used as input for the nonlinear dynamic analysis of the case-study structure. SIMBAD includes a total of 467 tri-axial accelerograms, consisting of two horizontal (X-Y) and one vertical (Z) components, generated by 130 worldwide seismic events The database includes shallow crustal earthquakes with moment magnitudes (M) ranging from 5 to 7.3 and epicentral distances R ≤ 35 km. The specific subset of records considered here provides a statistically significant number of strong-motion records of engineering relevance for the applications presented in this paper. Those records cover a wide range of magnitudes, source-to-site distance and soil types and are selected by first ranking the 467 records in terms of their PGA values (by using the geometric mean of the two horizontal components) and then keeping the component with the largest PGA value (for the 150 stations with highest mean PGA).

The spectral acceleration at the fundamental period of the hosting structure, $S_a(T_1)$, was the selected IM to calibrate the proposed loss-based control algorithm. To this aim, in each time-history analysis (i.e., for a given ground motion input), the MR damper is fed with a range of voltage values, always keeping the input voltage constant for the duration of the motion. Ten command voltages from 0 V to 2.25 V in 0.25 V steps are

considered. Around 1,500 dynamic analyses are performed in total. For each analysis, 9 different EDPs are recorded (for each voltage) and the optimal value of voltage u_{opt} – the one leading to the minimum expected loss as computed using Eq. (5) – is identified. The EDPs considered are: 1) peak displacement (over time) for each story; 2) peak inter-story drift ratio (over time) for each story, as the largest difference between the lateral displacements of two adjacent floors, divided by the height of the story (denoted as IDR_i for story *i*-th); and 3) peak acceleration (over time) for each story (denoted as PFA_i for story *i*-th).

Fig. 5 shows how the EDPs – IDR at the first story (Fig. 5a) and PFA at the third story (Fig. 5b) vary with the input voltage for two generic ground motion records. As could be anticipated, each EDP has a specific variation with the input voltage so that the voltage value minimizing each EDP is not necessarily the same for all EPDs. From the simulation results obtained, the optimum voltage value in terms of IDR is usually the maximum possible voltage (u_{max}) as shown in Fig. 5a. However the dependence of PFA with the input voltage is quite variable and the optimum voltage is strongly IM-dependent as illustrated in Fig. 5b. By combining these conflicting demands into a single performance variable, the proposed loss-based approach offers a powerful control tool.

The story-based approach defined in Eqs. (3-5) requires 1) that the replacement value of the entire building can be distributed among each story and each type of building components in the structure; and 2) damage functions relating the EDPs to the monetary loss of the entire story. Regarding point 1), for the case-study building used here, assumptions are made on how the replacement value is distributed among its stories and components. Specifically, it is assumed that the total value is uniformly distributed across all the stories. Each story's value is distributed into the three categories of components described above assuming the following value breakdown: (1) 0% for drift-sensitive structural components (for simplicity); (2) 50% for drift-sensitive non-structural components; and (3) 50% for acceleration-sensitive components. Regarding point 2), the first step is to define the damage states associated with the component. Definition of damage states is based on the courses of action that need to be taken after observing that damage state in the component. Fragility functions for each category of component are based on HAZUS. For illustrative purposes, only one damage state, corresponding to complete damage, is considered for generic non-structural components in office buildings. The fragility functions used for these components are shown in Fig. 6a (drift-sensitive) and 6b (acceleration-sensitive).

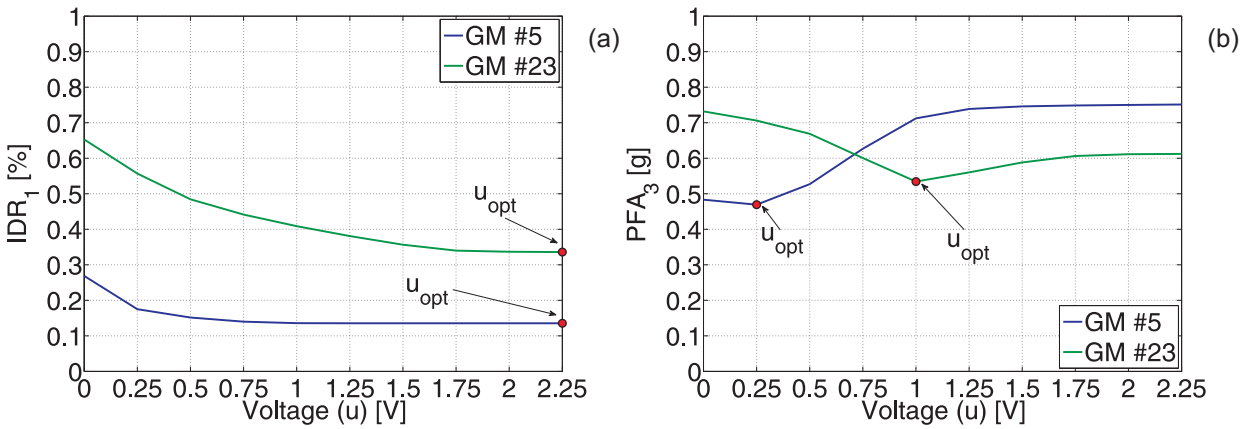

Fig. 5 - Example of EDPs vs voltage curves and optimal voltage values for two generic ground motion records: (a) IDR at the first story; (b) PFA at the third story.

Fig. 7a shows how the normalized expected loss ratio for two generic ground motion records varies witht the input voltage. From these curves, a single optimum input voltage can clearly be identified and recorded for each ground motion (and associated IM); Fig. 7b shows the optimal voltage as function of $S_a(T_1)$. The curve shown is obtained by fitting the cloud of points by robust regression. Each point represents the loss-optimum voltage value for a given ground motion (i.e. IM). This graph is key to calibrate the optimal control algorithm. It shows that for this particular case-study, for events with $S_a(T_1) \leq 0.25$g, the loss-optimum voltage to drive the

MR damper is the minimum value (0 V). For 0.25g < $S_a(T_1)$ < 0.7g, the optimum values are fitted to the relationship indicated in the figure, whereas for $S_a(T_1)$ ≥ 0.7g, the loss-optimum voltage input should be the maximum value (2.25 V).

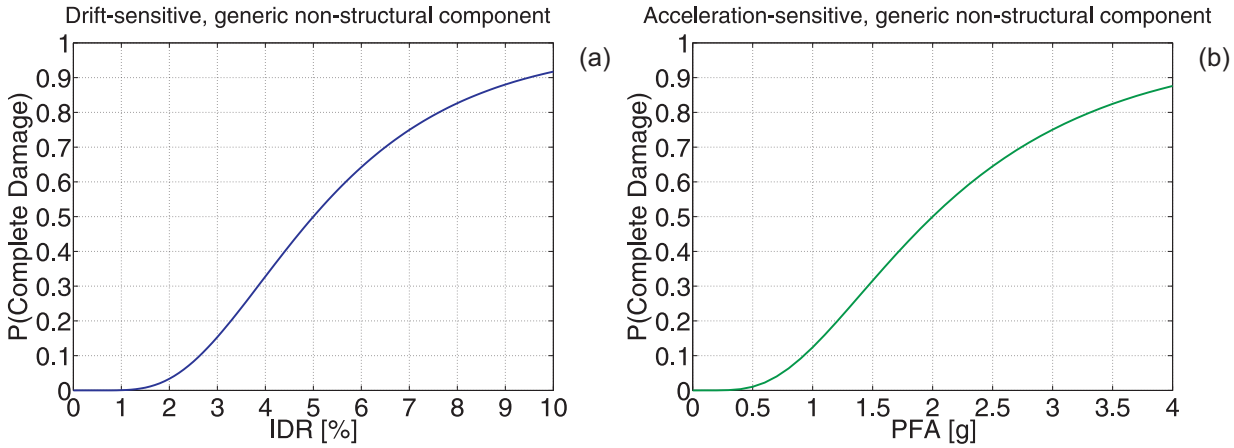

Fig. 6 - Fragility functions for complete damage for (a) drift-sensitive, generic non-structural component (in office buildings); and (b) acceleration-sensitive, generic non-structural component (in office buildings).

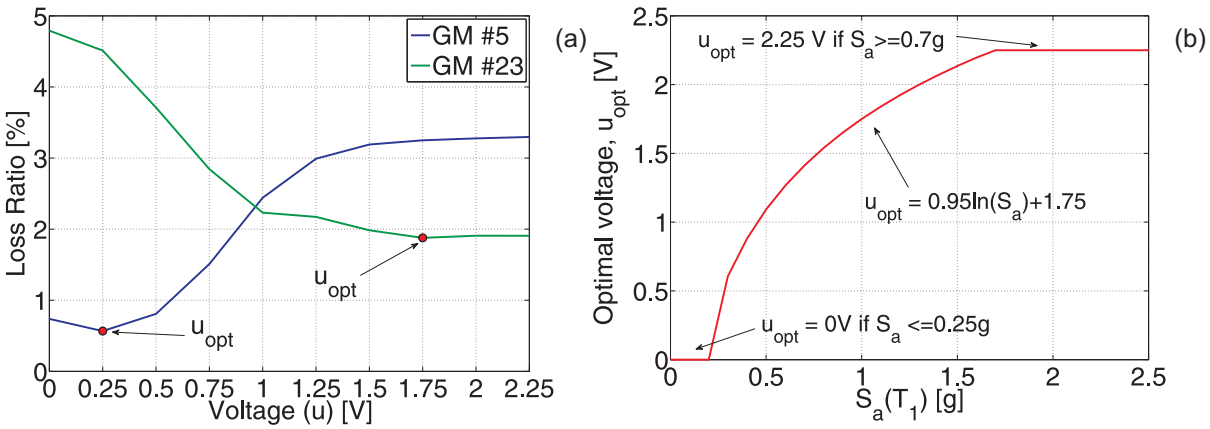

Fig. 7 - (a) Example of loss vs voltage curves and optimal voltage values for two generic ground motion records; (b) optimal control algorithm.

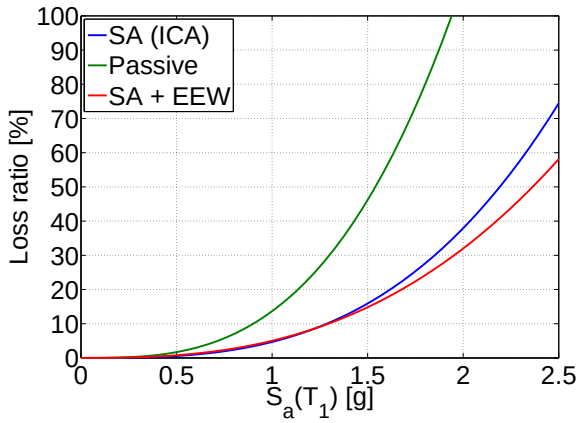

Fig. 8 - Comparison of different control algorithms for the case-study structure in terms of loss ratio vs IM.

Fig. 8 shows the loss ratio in terms of $S_a(T_1)$ for the three different control strategies described at the end of section 2. It illustrates how a loss-estimation framework allows control algorithms to be compared. For this case study, the best performing control strategy (in terms of loss) for all IM is the 'SA+EEW' one (red line). The 'SA ICA' (blue line) is a fairly close second, whereas the passive mode (green line) performs much more poorly. Therefore the proposed methodology ('SA+EEW') provides the best response of the structure (in terms of losses) compared to the chosen semi-active and passive strategies.

5. Conclusions

This paper shows how MR dampers can be integrated with an EEW system to control just-in-time the dynamic characteristics of a structure to achieve an optimal response against seismic forces. The "smart-passive" strategy sets the voltage to a constant optimum value for the duration of a given event. It is shown how this optimum value for a given event can be obtained in advance through a calibration process carried out once and for all using ground motion records. These are used as input for nonlinear dynamic analyses of the structure fitted with MR dampers. By varying the input voltage and recording relevant EDPs, the loss associated with a given ground motion and input voltage can be estimated and the loss-optimum input voltage to the MR damper can be identified.

The methodology is illustrated on a case-study based on a three-floor shear frame fitted with one MR damper between the ground floor and the first floor. It is shown how the loss estimation framework allows an overall optimum voltage value to be identified even though each EDP can be minimized by different voltage values.

The new SA+EEW strategy is proved to perform better (in terms of losses) against traditional control methodologies, leading to future potential research on the feasibility of the proposed control algorithm.

6. References

[1] A. Zollo, G. Festa, A. Emolo, and S. Colombelli, "Source Characterization for Earthquake Early Warning," *Encycl. Earthq. Eng.*, pp. 1–11, 2014.

[2] I. Iervolino, M. Giorgio, C. Galasso, and G. Manfredi, "Uncertainty in early warning predictions of engineering ground motion parameters: What really matters?," *Geophys. Res. Lett.*, vol. 36, no. 5, pp. 1–6, 2009.

[3] I. Iervolino, V. Convertito, and M. Giorgio, "Real-time risk analysis for hybrid earthquake early warning systems," *J. Earthq.*, pp. 1–20, 2006.

[4] I. Iervolino, C. Galasso, and G. Manfredi, "Preliminary investigation on integration of semi-active structural control and earthquake early warning," pp. 50–59, 2009.

[5] V. Convertito, I. Iervolino, A. Zollo, and G. Manfredi, "Prediction of response spectra via real-time earthquake measurements," *Soil Dyn. Earthq. Eng.*, vol. 28, no. 6, pp. 492–505, 2008.

[6] I. Iervolino, M. Giorgio, and G. Manfredi, "Expected loss-based alarm threshold set for earthquake early warning systems," *Earthq. Eng. Struct. Dyn.*, vol. 36, no. 9, pp. 1151–1168, Jul. 2007.

[7] I. Iervolino, "Performance-based earthquake early warning," *Soil Dyn. Earthq. Eng.*, vol. 31, no. 2, pp. 209–222, 2011.

[8] J. W. Baker, "An Introduction to Probabilistic Seismic Hazard Analysis (PSHA)," 2008.

[9] T. T. Soong and B. F. Spencer Jr, "Supplemental energy dissipation : state-of-the-art and state-of-the- practice," *Eng. Struct.*, vol. 24, pp. 243–259, 2002.

[10] S. J. Dyke, B. F. Spencer, M. K. Sain, and J. D. Carlson, "Modeling and control of magnetorheological dampers for seismic response reduction," *Smart Mater. Struct.*, vol. 5, no. 5, pp. 565–575, 1996.

[11] B. F. J. Spencer and S. Nagarajaiah, "State of the Art of Structural Control," *J. Struct. Eng.*, vol. 129, no. 7, pp. 845–856, 2003.

[12] D. A. Pohoryles and P. Duffour, "Adaptive control of structures under dynamic excitation using magnetorheological dampers: an improved clipped-optimal control algorithm," *J. Vib. Control*, no. April 2013, 2013.

[13] L. R. Barroso and S. Winterstein, "Probabilistic seismic demand analysis of controlled steel moment-resisting frame

structures," *Earthq. Eng. Struct. Dyn.*, vol. 31, no. 12, pp. 2049–2066, 2002.

[14] A. Occhiuzzi, M. Spizzuoco, and G. Serino, "Experimental analysis of magnetorheological dampers for structural control," *Smart Mater. Struct.*, vol. 12, no. 5, pp. 703–711, 2003.

[15] D. H. Wang and W. H. Liao, "Magnetorheological fluid dampers: a review of parametric modelling," *Smart Mater. Struct.*, vol. 20, no. 2, p. 023001, 2011.

[16] Y. Chae, J. M. Ricles, and R. Sause, "Modeling of a large-scale magneto-rheological damper for seismic hazard mitigation. Part II: Semi-active mode," *Earthq. Eng. Struct. Dyn.*, vol. 42, no. 5, pp. 687–703, Apr. 2013.

[17] L. M. Jansen and S. J. Dyke, "Semi-Active Control Strategies for MR Dampers: A Comparative Study," *J. Eng. Mech.*, vol. 126, no. 8, pp. 795–803, 2000.

[18] G. Maddaloni, N. Caterino, G. Nestovito, and A. Occhiuzzi, "Use of seismic early warning information to calibrate variable dampers for structural control of a highway bridge: evaluation of the system robustness," *Bull. Earthq. Eng.*, vol. 11, no. 6, pp. 2407–2428, Sep. 2013.

[19] C. M. Ramirez and E. Miranda, "Building-Specific Loss Estimation Methods & Tools for Simplified Performance-Based Earthquake Engineering," no. 171, p. 370, 2009.

[20] C. B. Haselton and G. G. Deierlein, "Assessing Seismic Collapse Safety of Modern Reinforced Concrete Moment-Frame Buildings," 2007.

[21] F. Jalayer and C. A. Cornell, "Alternative non-linear demand estimation methods for probability-based seismic assessments," *Earthq. Eng. Struct. Dyn.*, vol. 38, no. 8, pp. 951–972, Jul. 2009.

[22] H. Aslani and E. Miranda, "Fragility Assessment of Slab-Column Connections in Existing Non-Ductile Reinforced Concrete Buildings," *J. Earthq. Eng.*, vol. 9, no. 6, pp. 777–804, 2005.

[23] B. F. J. Spencer, S. J. Dyke, M. K. Sain, and J. D. Carlson, "Phenomenological Model for Magnetorheological Dampers," *J. Eng. Mech.*, vol. 123, no. 3, pp. 230–238, 1997.

[24] C. Smerzini, C. Galasso, M. Eeri, I. Iervolino, and R. Paolucci, "Ground Motion Record Selection Based on Broadband Spectral Compatibility."